JPET Fast Forward. Published on February 5, 2013 as DOI: 10.1124/jpet.113.203125

JPET #203125

In vitro–in vivo correlation of the inhibition potency of sodium-glucose cotransporter inhibitors in rat: a pharmacokinetic and pharmacodynamic modeling approach

Koji Yamaguchi, Motohiro Kato, Masayuki Suzuki, Hitoshi Hagita, Maiko Takada, Miho Ayabe, Yoshinori Aso, Masaki Ishigai, and Sachiya Ikeda

Research Division, Chugai Pharmaceutical Co., Ltd., 1-135 Komakado, Gotemba, Shizuoka 412-8513, Japan (K.Y., M.K., M.S., M.T., M.A., Y.A, M.I., S.I.)

Chugai Research Institute for Medical Science, Inc., 1-135 Komakado, Gotemba, Shizuoka 412-8513, Japan (H.H.)

Running title (60 characters including space): IVIVC for inhibition potency of SGLT inhibitors

Correspondence to: Koji Yamaguchi

Research Division, Chugai Pharmaceutical Co., Ltd., 1-135 Komakado, Gotemba, Shizuoka 412-8513, Japan

Telephone: +81-550-87-6708

Fax: +81-550-87-5397

E-mail: yamaguchikuj@chugai-pharm.co.jp

Numbers of the manuscript:

Text pages: 43

Figures: 6

Tables: 4

References: 36

Words in Abstract: 229

Words in Introduction: 593

Words in Discussion: 1653

Abbreviations: SGLT, sodium-glucose cotransporter; rSGLT, rat SGLT; mSGLT, mouse SGLT; PK-PD, pharmacokinetic and pharmacodynamic; GFR, glomerular filtration rate; $K_{m,\ SGLT1}$, Michaelis-Menten constant of SGLT1 for glucose; $K_{m,\ SGLT2}$, Michaelis-Menten constant of SGLT2 for glucose; $V_{max,\ SGLT1}$, maximum transport capacity of SGLT1 for glucose; $V_{max,\ SGLT2}$, maximum transport capacity of SGLT2 for glucose; $K_{i,\ SGLT1}$, inhibition constant for SGLT1; $K_{i,\ SGLT2}$, inhibition constant for SGLT2; $CL_{R,Glc}$, renal glucose clearance; AMG, α-methyl glucopyranoside; f_u, fraction unbound in rat serum; FE, fractional excretion of filtered glucose into urine; UGE, urinary glucose excretion; CV, coefficient of variation

Recommended sections: Drug Discovery and Translational Medicine

JPET Fast Forward. Published on February 5, 2013 as DOI: 10.1124/jpet.113.203125
This article has not been copyedited and formatted. The final version may differ from this version.

Abstract

In order to evaluate the relationship between the in vitro and in vivo potency of sodium-glucose cotransporter (SGLT) inhibitors, a pharmacokinetic and pharmacodynamic (PK-PD) study was performed using normal rats. A highly selective SGLT2 inhibitor, tofogliflozin, and four other inhibitors with different in vitro inhibition potency to SGLT2 and selectivity toward SGLT2 versus SGLT1 were used as test compounds, and the time courses for urinary glucose excretion (UGE) and the plasma glucose and compound concentrations were monitored after administration of the compounds. A PK-PD analysis of the UGE caused by SGLT inhibition was performed based on a nonlinear parallel tube model which took into consideration the consecutive reabsorption by different glucose transport properties of SGLT2 and SGLT1. The model adequately captured the time course of cumulative UGE caused by SGLT inhibition; then the in vivo inhibition constants (K_i) of inhibitors for both SGLT1 and SGLT2 were estimated. The in vivo selectivity toward SGLT2 showed a good correlation with the in vitro data ($r = 0.985$, $p < 0.05$), with in vivo K_i values for SGLT2 in the range of 0.3- to 3.4-fold the in vitro data. This suggests that in vitro inhibition potency to both SGLT2 and SGLT1 is reflected in vivo. Furthermore, the complementary role of SGLT1 to SGLT2 and how selectivity toward SGLT2 affects the inhibitory potency for renal glucose reabsorption were discussed using the PK-PD model.

Introduction

In normal animals and subjects, glucose is filtered at the glomerulus of the kidney and almost completely reabsorbed by sodium-glucose cotransporters (SGLT) expressed in the proximal tubules. Two isoforms of SGLT with different affinity to glucose are localized at different positions in the proximal tubule: a low-affinity and high-capacity transporter (SGLT2) is expressed in the convoluted tubule and a high-affinity and low-capacity transporter (SGLT1) is expressed in the straight tubule (**Turner and Moran, 1982; Hediger and Rhoads, 1994; Oulianova and Berteloot, 1996; Wright, 2001**). The glucosuria observed in SGLT2 knockout mice (**Vallon et al., 2011; Jurczak et al., 2011**) and in familial renal glucosuria patients (**Elsas and Rosenberg, 1969**) with SGLT2 mutation (**Magen et al., 2005**) indicates that SGLT2 plays a predominant role in renal glucose reabsorption in the kidney.

It has been reported that inhibiting SGLT increases urinary glucose excretion (UGE) and reduces blood glucose, which improves glycemic control in an insulin-independent manner (**Rossetti et al., 1987; Oku et al., 2000**). Accordingly, several SGLT inhibitors are currently under clinical development for type II diabetes treatment (**Abdul-Ghani et al., 2011; Kipnes, 2011**). Considering that two isoforms of SGLT with different properties contribute to renal glucose reabsorption and that SGLT1 is expressed in not only the kidney but also the small intestine (**Hediger and Rhoads, 1994**), the inhibition potency to each transporter would be an important factor in efficacy and safety. Although both SGLT1 and SGLT2 in the kidney can be targets for type II diabetes treatment, most SGLT inhibitors being developed have high selectivity toward

JPET Fast Forward. Published on February 5, 2013 as DOI: 10.1124/jpet.113.203125
This article has not been copyedited and formatted. The final version may differ from this version.

SGLT2 versus SGLT1, in order to avoid some possible adverse events that may be caused by SGLT1 inhibition (**Jabbour and Goldstein, 2008**). SGLT2 inhibitors are known to exhibit different levels of glucosuric potency **(List and Whaley, 2011)** and both the in vitro SGLT2 inhibition constant and selectivity toward SGLT2 would be important factors in the in vivo inhibitory effect on renal glucose reabsorption. Moreover, pharmacokinetic properties such as bioavailability and half-life would also be a considerable issue for in vivo effectiveness. As described above, many factors affect the in vivo efficacy of an SGLT inhibitor, making it difficult to predict in vivo efficacy from in vitro data or, in this specific case, to know how in vitro inhibition potency to SGLT2 and selectivity toward SGLT2 would be reflected in vivo.

The purpose of this study is to evaluate the in vitro–in vivo relationship of the inhibition constant (K_i) of SGLT inhibitors. Tofogliflozin is a highly potent and selective SGLT2 inhibitor (**Suzuki et al., 2012; Ohtake et al., 2012**) and is currently in a Phase III trial for type II diabetes mellitus treatment. We used tofogliflozin and other inhibitors with different in vitro inhibition potency to SGLT2 and selectivity toward SGLT2 as the test compounds, and carried out PK-PD studies of them using normal rats. We previously developed a mechanism-based PK-PD model in which the different glucose transport properties between SGLT1 and SGLT2 were considered (**Yamaguchi et al., 2011**). The model was able to describe the plasma glucose-dependent UGE in rats; moreover, it could estimate the in vivo inhibition constants of SGLT1 and SGLT2 for phlorizin, which has less selectivity toward SGLT2. In the present study, we used the PK-PD

JPET Fast Forward. Published on February 5, 2013 as DOI: 10.1124/jpet.113.203125
This article has not been copyedited and formatted. The final version may differ from this version.

model to estimate the in vivo K_i of SGLT inhibitors by analyzing the relationship between UGE and plasma inhibitor concentration and then analyzed the in vitro–in vivo relationship for K_i. Furthermore, a simulation study was performed in order to understand how selectivity toward SGLT2 affects the inhibitory effect on renal glucose reabsorption under euglycemic and hyperglycemic conditions.

JPET Fast Forward. Published on February 5, 2013 as DOI: 10.1124/jpet.113.203125
This article has not been copyedited and formatted. The final version may differ from this version.

Methods

Chemicals. (1*S*, 3'*R*, 4'*S*, 5'*S*, 6'*R*)-6-[(4-ethylphenyl)methyl]-3',4',5',6'-tetrahydro -6'-(hydroxymethyl)-spiro[isobenzofruran-1 (3*H*), 2'-[2*H*] pyran]-3',4',5'-triol (tofogliflozin) (Ohtake et al., 2012), 2-[(4-methoxyphenyl)methyl]phenyl 6-*O*-ethoxycarbonyl-β-D-glucopyranoside (sergliflozin) (**Katsuno et al., 2007**), 2-[(4-methoxyphenyl)methyl]phenyl-β-D-glucopyranoside (sergliflozin-A, an active form of sergliflozin), 3-(benzo[*b*]furan-5-yl)-2',6'-dihydroxy-4'-methylpropiophenone-2'-*O*-(6-*O*-methoxycarbonyl)-β-D-glucopyranoside (T-1095) (**Oku et al., 1999**), 3-(benzo[*b*]furan-5-yl)-2',6' -dihydroxy-4'-methylpropiophenone-2'-*O*-β-D- glucopyranoside (T-1095A, an active form of T-1095) (Oku et al., 1999), and (2S,3R,4R,5S,6R)-2-(3-(4-ethylbenzyl)-(phenyl)-6-hydroxymethyl-tetrahydro-2H-pyran-3,4,5-triol (BMS, a patent compound of Bristol-Myers Squibb Pharmaceutical Co.) (**Ellsworth et al., 2001; Deshpande et al., 2012**) were synthesized in Chugai Pharmaceutical Co., Ltd., and the chemical structures of the compounds are shown in **Fig. 1**. Phlorizin and α-methyl-D-glucopyranoside (AMG) were purchased from Sigma-Aldrich (St. Louis, MO, USA), and α-methyl-D-[^{14}C] glucopyranoside ([^{14}C]-AMG) was purchased from General Electronic Company (Tokyo, Japan).

Animals. Male Sprague-Dawley rats were purchased from Japan SLC Inc. (Shizuoka, Japan) and used for PK-PD studies at 8 weeks old. Male Wistar rats purchased from Japan SLC Inc. and male db/db mice (BKS.Cg - +Lepr^{db}/+Lepr^{db}/Jcl) purchased from Clea Japan Inc. (Tokyo, Japan) were used for cloning rat and mouse SGLTs. These animals were housed under a 12-h/12-h light/dark cycle (lights on 7:00 AM–7:00

JPET Fast Forward. Published on February 5, 2013 as DOI: 10.1124/jpet.113.203125
This article has not been copyedited and formatted. The final version may differ from this version.

PM) with controlled room temperature (20–26°C) and humidity (35–75%) and were allowed *ad libitum* access to a diet of laboratory chow (CE-2 pellets; Clea Japan) and water. Care of the animals and the protocols were performed in accordance with the "Guidelines for the Care and Use of Animals at Chugai Pharmaceutical Co., Ltd." and were approved by the Ethics Committee for Treatment of Laboratory Animals at Chugai Pharmaceuticals.

Inhibition study of AMG uptake using cells expressing rat and mouse SGLTs. In vitro inhibition studies using cells expressing rat SGLT1 (rSGLT1), rat SGLT2 (rSGLT2), mouse SGLT1 (mSGLT1), and mouse SGLT2 (mSGLT2) were performed by the method previously reported (**Suzuki et al., 2012**), as follows. Rat and mouse SGLTs cDNA was amplified with total RNA isolated from the kidney or small intestine of a Wistar rat or a db/db mouse. PCR primers were designed from published sequences (GenBank accession number: NM001107229 (rSGLT1), NM022590 (rSGLT2), BC003845 (mSGLT1), AY033886 (mSGLT2)). The sequences of PCR primers used were ACCTCGAGAACTCAAAAGCAGTATAAGG and ACCGATATCACATCTTTTATCCGAATGAG for rSGLT1, AACTCAAAAGCAGTATAAGG and ACATGCCCTGGTTGCAACTC for rSGLT2, ACCCTCGAGATGGACAGTAGCACCTTGAG and ACCGATATCAGGGCTCAGGCAAAATAGGC for mSGLT1 and ACCCTCGAGATGGAGCAACACGTAGAGGC and ACCGAATTCACACCCTCGACTTTATGCAT for mSGLT2. Experimental conditions for PCR with KOD Plus (TOYOBO Co., Osaka, Japan) were as follows: 94°C for 2 min; 35 cycles of 94°C for 15 s, 58°C for 30 s and 68°C for 3 min. Expression plasmids

JPET Fast Forward. Published on February 5, 2013 as DOI: 10.1124/jpet.113.203125
This article has not been copyedited and formatted. The final version may differ from this version.

containing rat and mouse SGLTs were prepared by ligating amplified cDNA fragments into the multi-cloning site of pcDNA3.1(–) (Life Technologies Co. [Invitrogen], Grand Island, NY, USA). The expression plasmids containing mSGLT1 and mSGLT2 cDNA fragment were transfected into Chinese hamster ovary-K1 cells (CHO; American Type Culture Collection [ATCC]). Clones stably expressing each SGLT were used for the AMG uptake assay. The expression plasmids containing rSGLT1 and rSGLT2 cDNA fragments were transfected into African green monkey SV40-transfected kidney fibroblast cells (COS-7; ATCC), and the cells transiently expressing each SGLT were used for the AMG uptake assay.

For the AMG uptake assay, the cells expressing each SGLT were cultured in 96-well plates for 2 or 3 days and washed twice with sodium-free buffer (140 mM choline chloride, 2 mM KCl, 1 mM $CaCl_2$, 1 mM $MgCl_2$, 10 mM HEPES/Tris pH7.4). The cells were then incubated in sodium-free buffer or sodium buffer (140 mM NaCl, 2 mM KCl, 1 mM $CaCl_2$, 1 mM $MgCl_2$,10 mM HEPES/Tris pH7.4) each containing 1mM AMG mixture (non-radiolabeled AMG and [^{14}C]-AMG) at 37°C for 45 min. Sodium-dependent AMG uptake was calculated by subtracting the radioactivity detected in cells incubated in the sodium-free buffer from the radioactivity detected in the cells incubated in the sodium buffer. IC_{50} values of SGLT inhibitors were calculated with the empirical four-parameter model fitting of XLfit (IDBS, Guildford, UK) and were indicated as mean values of 2 to 4 independent experiments. Selectivity toward SGLT2 versus SGLT1 was calculated by dividing IC_{50} for SGLT1 by that for SGLT2.

Rat serum protein binding assay. Rat serum protein binding of each test compound was measured

JPET Fast Forward. Published on February 5, 2013 as DOI: 10.1124/jpet.113.203125
This article has not been copyedited and formatted. The final version may differ from this version.

using the equilibrium dialysis method. 100 mM potassium phosphate buffered solution (pH 7.4) was added to a receptor chamber, and rat serum containing a test compound (final concentration: 100 ng/ml) was added to a donor chamber. The equilibrium dialysis apparatus was incubated in a shaking bath for 24 h at 37°C. After incubation, buffer and serum samples were collected, and the test compound concentrations were measured using LC-MS/MS. The fraction unbound in serum (f_u) was calculated using the equation below:

$$f_u = \frac{C_{buffer}}{C_{serum}}$$

where C_{buffer} and C_{serum} were test compound concentration in buffer and serum, respectively. f_u was calculated as the mean value of three experiments. The f_u values of tofogliflozin (**Suzuki et al., 2012**) and phlorizin (**Yamaguchi et al., 2011**) were cited from previous reports.

PK-PD studies of SGLT inhibitors in rats. Under ether anesthesia, polyethylene cannulae were placed in the femoral artery and vein of each rat, and a silicon cannula was placed in the bladder. After surgery, the rats were housed in Bollman cages (Natsume Seisakusho Co., Ltd., Tokyo, Japan). The dosing solutions were administered as a bolus through the femoral venous cannula or by oral gavage. The composition of the dosing solution for each drug is summarized in **Table 1**. The number of animals was 3 or 4 for each dosing group. Blood samples (200 μl) were collected from the arterial cannula before administration and at 2 (only for intravenous administration), 5, 15, 30, 60, 120, 240, and 480 min after administration. Urine samples were collected from the bladder cannula at intervals of 1 to 2 h. The sampling

of urine was initiated 1 h before administration and terminated 8 h after administration. The bladder was washed with 1 ml of saline in order to collect urine completely at each sampling point. The glucose concentrations in plasma and urine samples were determined using a Glucose CII-Test Wako kit (Wako Pure Chemical Industries, Ltd., Osaka, Japan). The PK-PD data of phlorizin was cited from a previous report (**Yamaguchi et al., 2011**).

Measurement of test compounds using LC-MS/MS. To 50 μl of plasma sample were added 20 μl of internal standard solution and 20 μl of blank solvent for standard solution, and mixed. Then 500 μl of distilled water and 2 ml of diethyl ether were added to the mixture, and mixed for 5 min. The mixture was centrifuged at 3,000 rpm for 10 min (4°C). The organic phase was collected and evaporated under a nitrogen stream. To the residue was added 50 μl of acetonitrile/10 mM ammonium acetate (4:6, v/v) to prepare an HPLC sample. Standard samples for calibration were prepared by the same method using standard solutions instead of blank solvent. Phenytoin (500 ng/ml) was used as the internal standard for tofogliflozin, BMS, and sergliflozin-A, and indomethacin (200 ng/ml) was used as the internal standard for T-1095A.

The HPLC sample was injected at a volume of 20 μl and the drug concentration was measured using the following LC-MS/MS method. The LC-MS/MS analysis was carried out by coupling a liquid chromatography system to an API300 mass spectrometer (Applied Biosystems/MDS SCIEX, Concord, ON, Canada). The HPLC apparatus consisted of a pump (LC-10AD; Shimadzu Co., Kyoto, Japan) and an auto

JPET Fast Forward. Published on February 5, 2013 as DOI: 10.1124/jpet.113.203125
This article has not been copyedited and formatted. The final version may differ from this version.

injector (SIL-HTC; Shimadzu Co.). A CAPCELL PAK C18 column (UG120, 5 μm, 2.0 × 150 mm; Shiseido Co., Ltd., Tokyo, Japan) was used as the analytical column. The mobile phase was methanol/10 mM ammonium acetate (4:6, v/v) at a flow rate of 0.2 ml/min. The HPLC elute was introduced into the source using a TurboIonSpray® interface (Applied Biosystems/MDS SCIEX) and the mass spectrometer was operated in positive ion mode for tofogliflozin, BMS, and sergliflozin-A, and in negative ion mode for T-1095A. Selected ions were m/z 267.1 (daughter ion of 387.1) for tofogliflozin, m/z 119.1 (daughter ion of 376.1) for BMS, m/z 180.1 (daughter ion of 394.2) for sergliflozin-A, m/z 295.0 (daughter ion of 456.9) for T-1095A, m/z 182.1 (daughter ion of 253.1) for phenytoin, and m/z 312.0 (daughter ion of 355.8) for indomethacin. Run cycles of measurements were set at 10 min (tofogliflozin and BMS), 6 min (T-1095A), and 13 min (sergliflozin-A). The linear calibration curve for each compound using peak area was obtained in the range of 10–2,000 ng/ml for tofogliflozin, 1–1,000 ng/ml for BMS, 30–2,000 ng/ml for sergliflozin-A, and 3–300 ng/ml for T-1095A, with weighting 1/y.

Estimation of renal clearance and average plasma concentration. The renal glucose clearance ($CL_{R,Glc}$) during each urine sampling period was estimated using the following equation:

$$CL_{R,Glc} = \frac{C_{U,Glc} \cdot V}{AUC_{Glc}}$$

where $C_{U,Glc}$ is the concentration of glucose in urine, V is the urine volume, and AUC_{Glc} is the area under the time-plasma concentration curve for glucose during the corresponding urine-sampling period (τ). The average plasma concentrations of glucose ($C_{Av,Glc}$) and test compound ($C_{Av,Drug}$) were also estimated by the

JPET Fast Forward. Published on February 5, 2013 as DOI: 10.1124/jpet.113.203125
This article has not been copyedited and formatted. The final version may differ from this version.

following equations:

$$C_{Av,Glc} = \frac{AUC_{Glc}}{\tau},\ C_{Av,Drug} = \frac{AUC_{Drug}}{\tau}$$

where AUC_{Drug} is the area under the time-plasma concentration curve for the test compound during the corresponding urine-sampling period (τ).

PK-PD model for the effect of an SGLT inhibitor on renal glucose transport. The previously developed PK-PD model (**Yamaguchi et al., 2011**) was used in this study, and the details are shown below. In order to express the renal glucose reabsorption and the inhibitory effect of an SGLT inhibitor, the following concepts were assumed in the model: 1) first, the filtered plasma glucose is reabsorbed by SGLT2, and then the remainder is reabsorbed by SGLT1; 2) the flow rate in the proximal tubule is the same as the glomerular filtration rate (GFR); 3) the glucose concentration in the proximal tubule is altered only by the reabsorption mediated by SGLTs; 4) the glucose reabsorption process mediated by SGLTs is expressed by a nonlinear parallel tube model; 5) the inhibitor concentration in the proximal tubule is the same as that in plasma and shows a constant value; and 6) an inhibitor competitively inhibits the glucose transport mediated by SGLTs. A schematic representation of the PK-PD model is shown in **Fig. 2**. The glucose transport in the proximal tubule at time *t* is expressed by the following equations:

$$C_{in2}(t) - C_{out2}(t) + K_{m,SGLT2} \cdot (1 + \frac{C(t)}{K_{i,SGLT2}}) \cdot (\ln C_{in2}(t) - \ln C_{out2}(t)) = \frac{V_{\max,SGLT2}}{GFR} \qquad \text{Eq. 1}$$

$$C_{in1}(t) - C_{out1}(t) + K_{m,SGLT1} \cdot (1 + \frac{C(t)}{K_{i,SGLT1}}) \cdot (\ln C_{in1}(t) - \ln C_{out1}(t)) = \frac{V_{\max,SGLT1}}{GFR} \qquad \text{Eq. 2}$$

JPET Fast Forward. Published on February 5, 2013 as DOI: 10.1124/jpet.113.203125
This article has not been copyedited and formatted. The final version may differ from this version.

$C_{in2}(t) = C_{P,Glc}(t), \quad C_{out2}(t) = C_{in1}(t)$

where Eqs. 1 and 2 express the glucose transport at the compartments of SGLT2 and SGLT1, respectively. $C_{in2}(t)$ is the glucose concentration just after filtration at time t, which is equal to the glucose concentration in plasma at time t ($C_{P,Glc}(t)$). $C_{out2}(t)$ is the glucose concentration at the end of the SGLT2 compartment and is equal to $C_{in1}(t)$, which is the concentration at the entrance of the SGLT1 compartment at time t . $C_{out1}(t)$ is the concentration at the end of the SGLT1 compartment at time t. $C(t)$ is the plasma concentration of an inhibitor at time t after administration. $K_{i,\,SGLT1}$ and $K_{i,\,SGLT2}$ are the inhibition constants of an inhibitor for SGLT1 and SGLT2, respectively. The plasma concentration-time profile of an inhibitor, $C(t)$, is assumed to be expressed based on a 2-compartment model. Then the following equation was obtained:

$$C(t) = \frac{Dose}{V_1} \cdot \left(\frac{(k_{21} - \alpha)}{(\beta - \alpha)} \cdot \exp(-\alpha \cdot t) + \frac{(k_{21} - \beta)}{(\alpha - \beta)} \cdot \exp(-\beta \cdot t) \right)$$

$$\alpha = \frac{(k_{10} + k_{12} + k_{21}) + \sqrt{(k_{10} + k_{12} + k_{21})^2 - 4 \cdot k_{21} \cdot k_{10}}}{2}$$

$$\beta = \frac{(k_{10} + k_{12} + k_{21}) - \sqrt{(k_{10} + k_{12} + k_{21})^2 - 4 \cdot k_{21} \cdot k_{10}}}{2}$$

where *Dose* is the administration dose, V_1 is the distribution volume of the central compartment, k_{12} and k_{21} are the rate constants from central to peripheral and from peripheral to central compartment, respectively, k_{10} is the elimination rate constant from the central compartment, and α and β are the elimination rate constants at α- and β-phase, respectively.

The renal glucose clearance at time t ($CL_{R,Glc}(t)$) was estimated by the following equation:

JPET Fast Forward. Published on February 5, 2013 as DOI: 10.1124/jpet.113.203125
This article has not been copyedited and formatted. The final version may differ from this version.

$$CL_{R,Glc}(t) = GFR \cdot \frac{C_{out1}(t)}{C_{P,Glc}(t)} \quad \text{Eq. 3}$$

The cumulative glucose amount excreted in urine at time t ($Q_{U,Glc}$ (t)) was estimated by the following equation:

$$Q_{U,Glc}(t) = \int_0^t CL_{R,Glc}(t) \cdot C_{P,Glc}(t)dt \quad \text{Eq. 4}$$

Estimation of pharmacokinetic parameters. The plasma concentration-time profile of each test compound after intravenous administration to rat was analyzed based on the 2-compartment model using WinNonlin Ver. 5.0 software (Pharsight Co., Mountain View, CA, USA).

PK-PD analysis. The time course of cumulative glucose excreted after intravenous administration of an SGLT inhibitor was analyzed based on the PK-PD model using the following procedure. The $C(t)$ was simulated based on the 2-compartment model using the PK parameters obtained from the present PK analysis. The $C_{P,Glc}$ (t) was calculated by linear interpolation between observed values. Next, the fixed values ($K_{m,\ SGLT1}$, $K_{m,\ SGLT2}$, $V_{max,\ SGLT1}$, $V_{max,\ SGLT2}$, and GFR) obtained from the previous study (**Yamaguchi et al., 2011**) and simulated values ($C(t)$ and $C_{P,Glc}(t)$) were substituted into Eqs. 1–4. Then the values for $Q_{U,\ Glc}$ (t) observed in the PK-PD study were fitted to Eq. 4 in order to estimate the parameters, rat $K_{i,\ SGLT1}$ and rat $K_{i,\ SGLT2}$. Curve-fitting procedures were performed using a nonlinear least square regression program, MULTI (**Yamaoka et al., 1981**), with weighting 1/y.

In order to compare in vivo K_i with in vitro IC_{50}, the in vitro IC_{50} values were transformed to K_i values using the Cheng-Prusoff relationship (**Cheng and Prusoff, 1973**) as follows:

JPET Fast Forward. Published on February 5, 2013 as DOI: 10.1124/jpet.113.203125
This article has not been copyedited and formatted. The final version may differ from this version.

$$K_{\text{i, SGLT1}} = IC_{50,SGLT1} \Big/ \left(1 + \frac{S}{K_{m,SGLT1}}\right)$$

$$K_{\text{i, SGLT2}} = IC_{50,SGLT2} \Big/ \left(1 + \frac{S}{K_{m,SGLT2}}\right)$$

where S means AMG concentration (1 mM) used in the in vitro SGLT inhibition study. Selectivity toward SGLT2 versus SGLT1 was calculated by dividing $K_{\text{i, SGLT1}}$ by $K_{\text{i, SGLT2}}$.

Sensitivity analysis. In order to understand the relationship between selectivity toward SGLT2 and the effect on UGE, a simulation study was performed using the present PK-PD model. In the simulation, the PD parameters relating to renal glucose transport were used (**Table 2**), and it was assumed that $K_{\text{i,SGLT2}}$ of an SGLT inhibitor was 1 nM and that the selectivity toward SGLT2 was in the range of 1 to 1,000. In addition, no inhibition of SGLT1 (infinite selectivity toward SGLT2) was also assumed. $CL_{\text{R,Glc}}$ values were calculated under a static SGLT inhibitor concentration and at plasma glucose levels of 1, 2, or 3 mg/ml.

JPET Fast Forward. Published on February 5, 2013 as DOI: 10.1124/jpet.113.203125
This article has not been copyedited and formatted. The final version may differ from this version.

Results

In vitro IC_{50} of SGLT inhibitors. The IC_{50} values of test compounds determined from the AMG uptake assays are shown in **Table 3**. The IC_{50} values for rSGLT2 of test compounds were in the range of 15 to 48 nM, and those for rSGLT1 were in the range of 970 to 27,000 nM. IC_{50} values for mSGLT2 were in the range of 5.0 to 17 nM, and those for mSGLT1 were in the range of 96 to 6,900 nM. Test compounds showed a large variety in IC_{50} for mSGLT1 and rSGLT1 as compared with mSGLT2 and rSGLT2. Of the test compounds, tofogliflozin exhibited the lowest IC_{50} for both mSGLT2 (IC_{50}: 5.0 nM) and rSGLT2 (IC_{50}: 15 nM). Tofogliflozin, BMS, and sergliflozin-A showed relatively high selectivity toward SGLT2 (rat: more than 170, mouse: more than 150) while T-1095A and phlorizin showed less selectivity (rat: less than 20, mouse: less than 19). The rank orders of IC_{50} values for both SGLT1 and SGLT2 and of selectivity toward SGLT2 in rat were the same as those in mouse.

***$CL_{R,Glc}$* after administration of SGLT inhibitors.** The relationship between $CL_{R,Glc}$ and $C_{Av,Drug}$ after administration of test compounds is plotted in **Fig. 3**. Tofogliflozin, BMS, and sergliflozin were administered intravenously and orally, and the plots obtained from both administration routes are overlapped for each compound (**Figs. 3a–3c**). The regression curve was estimated for each test compound using the plots of $CL_{R,Glc}$ values that were in the range of 50 to 400 ml/h/kg, and using the following equation: $CL_{R,Glc} = slope \bullet \ln(C_{Av,Drug}) + a$

The slopes of the regression curves for less selective SGLT2 inhibitors (T-1095A and phlorizin) were

JPET Fast Forward. Published on February 5, 2013 as DOI: 10.1124/jpet.113.203125
This article has not been copyedited and formatted. The final version may differ from this version.

steeper than those for highly selective ones (tofogliflozin, BMS, and sergliflozin-A).

PK-PD analysis of SGLT inhibitors for renal glucose transport. The effect of an SGLT inhibitor on UGE after intravenous administration was analyzed based on the PK-PD model. The plasma concentration-time profile of each compound was suitably expressed using the 2-compartment model (**Fig. 4**), and the estimated parameters were summarized in **Table 4**. Using the fixed PD parameters relating to glucose transport (**Table 2**) (**Yamaguchi et al., 2011**) and simulated plasma concentrations of compound and glucose, the curve-fitting of cumulative UGE for each compound was performed based on the PK-PD model. The cumulative UGE of each test compound was suitably described by the present model (**Fig. 4**); then $K_{i,SGLT1}$ and $K_{i,SGLT2}$ were estimated (**Table 3**).

In vitro–in vivo relationship of K_i of SGLT inhibitors. The relationship between in vitro and in vivo K_i values of SGLT inhibitors was analyzed using rat data. In vitro IC_{50} values for SGLT1 and SGLT2 were transformed to K_i values using the Cheng-Prusoff relationship (**Cheng and Prusoff, 1973**), and in vivo K_i values were corrected by f_u. The relationship between in vitro K_i estimated using Cheng-Prusoff relationship and in vivo $K_i \times f_u$ is shown in **Fig. 5a**. The in vivo $K_{i,\,SGLT2} \times f_u$ values were in the range of 0.3- to 3.4-fold the in vitro data. The in vivo $K_{i,\,SGLT1} \times f_u$ values were in the range of 0.3- to 2.5-fold the in vitro data for three of four compounds and within 8-fold for one compound. Also, the in vivo $K_{i,\,SGLT2} \times f_u$ values of test compounds were comparable to the in vitro data previously reported: in vitro $K_{i,\,SGLT2}$ values of tofogliflozin, sergliflozin, and phlorizin were 14.9 nM (**Suzuki et al., 2012**), 17.1 nM (**Fujimori et al.,**

JPET Fast Forward. Published on February 5, 2013 as DOI: 10.1124/jpet.113.203125
This article has not been copyedited and formatted. The final version may differ from this version.

2009), and 39.4 nM **(Suzuki et al., 2012**), respectively. Moreover, there was a good correlation between in vitro and in vivo selectivity toward SGLT2 ($r = 0.985$, $p < 0.05$) (**Fig. 5b**).

Sensitivity analysis. In order to understand how the selectivity toward SGLT2 of an SGLT inhibitor affects its inhibition of renal glucose reabsorption, a sensitivity analysis was performed: the fractional excretion of filtered glucose (FE) was simulated assuming 1 nM of $K_{i,\ SGLT2}$ value, different selectivity toward SGLT2, and several plasma glucose levels. In the case of euglycemic condition (1 mg/ml), the threshold inhibitor concentration which causes more than 0.1% of FE was 3.0 nM when selectivity was 1, and 6.5–8.0 nM when selectivity was in the range of 10 to infinity (**Fig. 6a**). The threshold concentration increased as selectivity toward SGLT2 increased. In the case of hyperglycemic condition (2 mg/ml), the threshold concentrations for different levels of selectivity toward SGLT2 were comparable, with values in the range of 1.5 to 2.0 nM (**Fig. 6b**).

Under euglycemic condition, FE values showed a broad range between the different levels of selectivity toward SGLT2, with high selectivity causing a low FE value; FE value at a drug concentration of 1,000 nM was 96.0% when selectivity was 1, and was 53.8% when selectivity was infinity (**Fig. 6a**). Under hyperglycemic condition, on the other hand, the difference in FE between compounds with different levels of selectivity was slight; FE value at a drug concentration of 1,000 nM and at plasma glucose of 2 mg/ml was 96.2% when selectivity was 1, and was 76.0% when selectivity was infinity (**Fig. 6b**); and FE value at a drug concentration of 1,000 nM at plasma glucose of 3 mg/ml was 96.3% when selectivity was 1, and

JPET Fast Forward. Published on February 5, 2013 as DOI: 10.1124/jpet.113.203125
This article has not been copyedited and formatted. The final version may differ from this version.

was 83.6% when selectivity was infinity (**Fig. 6c**). The difference in FE got smaller as plasma glucose concentration increased.

JPET Fast Forward. Published on February 5, 2013 as DOI: 10.1124/jpet.113.203125
This article has not been copyedited and formatted. The final version may differ from this version.

Discussion

In the present study, a PK-PD analysis was performed based on a nonlinear parallel tube model, in which different properties in glucose transport between SGLT1 and SGLT2 were considered, in order to estimate in vivo K_i values and selectivity toward SGLT2 of SGLT inhibitors. The present PK-PD model was applied to SGLT inhibitors with different in vitro IC_{50} values and selectivity toward SGLT2 and could suitably express their time courses of UGE after administration (**Fig. 4**). We previously reported that the PK-PD model could express the plasma glucose concentration-dependent renal glucose excretion and the inhibitory effect of a less selective inhibitor, phlorizin, on renal glucose reabsorption in normal rat (**Yamaguchi et al., 2011**). In the present study, it was found that this model could be used to analyze the effect of other inhibitors including highly selective SGLT2 inhibitors such as tofogliflozin. The in vivo $K_i \times f_u$ values for SGLT1 and SGLT2 estimated using the present PK-PD model were comparable to the in vitro values (**Fig. 5**a). Moreover, the in vivo selectivity toward SGLT2 showed a good correlation with that in vitro (**Fig. 5b**). These results suggest that in vitro inhibition potency is reflected in vivo. Although plasma and proximal tubular drug concentrations were assumed to be equal in the analysis, the assumption would not reflect the actual in vivo situation because of renal secretion or reabsorption of a drug; for example, when renal reabsorption of a drug occurs, the estimated inhibition constant based on plasma drug concentration would be higher than that based on the actual tubular concentration. A more accurate in vitro-in vivo relationship for inhibition potency might be obtained by considering tubular drug

JPET Fast Forward. Published on February 5, 2013 as DOI: 10.1124/jpet.113.203125
This article has not been copyedited and formatted. The final version may differ from this version.

concentration.

When designing a potent SGLT2 inhibitor with specificity for a target organ, not only inhibition potency to SGLT2 but also selectivity toward SGLT2 are important indexes at the preclinical drug discovery stage. However, little is known of how the selectivity toward SGLT2 of a compound affects its inhibition potency for renal glucose reabsorption. In the present study, $CL_{R,Glc}$ was used to express the inhibitory effect of SGLT inhibitors on renal glucose reabsorption in order to evaluate the in vivo inhibition potency. As shown in **Fig. 3**, each inhibitor enhanced $CL_{R,Glc}$ as its plasma concentration increased, suggesting the plasma concentration-dependency of the inhibitory effect of SGLT inhibitors. The slope of the regression lines for the relationship between $CL_{R,Glc}$ and plasma inhibitor concentration obtained from highly selective SGLT2 inhibitors (tofogliflozin, BMS, and sergliflozin-A) was gradual compared with that from less selective ones (T-1095A and phlorizin). Moreover, the maximum enhancing efficacy for $CL_{R,Glc}$ of highly selective inhibitors was lower than that of less selective ones. These facts suggest that highly selective SGLT2 inhibitors have a milder inhibitory effect on renal glucose reabsorption than less selective ones in euglycemic rats. Some investigators reported the same trend: a less selective SGLT inhibitor, phlorizin, showed complete inhibition of renal glucose reabsorption in human (**Chasis et al., 1933**) and dog (**Silverman et al., 1970**), but the highly selective SGLT2 inhibitors, dapagliflozin (**Komoroski et al., 2009**) and sergliflozin (**Hussey et al., 2010**), exhibited less than 50% inhibition in human.

As described above, it seems obvious that selectivity toward SGLT2 could affect the inhibition

JPET Fast Forward. Published on February 5, 2013 as DOI: 10.1124/jpet.113.203125
This article has not been copyedited and formatted. The final version may differ from this version.

potency of a compound for renal glucose reabsorption. For a further understanding of the relationship between selectivity toward SGLT2 and inhibition potency for renal glucose reabsorption, a simulation study based on the PK-PD model was performed assuming several levels of selectivity toward SGLT2 under euglycemic and hyperglycemic conditions. The simulation results indicated that the inhibition potency of a highly selective SGLT2 inhibitor for renal glucose reabsorption was milder than that of a less selective one under euglycemic condition (**Fig. 6a**). $CL_{R,\,Glc}$ observed in the present study (**Fig. 3**) and previous reports for UGE in the presence of SGLT2 selective and less selective inhibitors (**Chasis et al., 1933; Komoroski et al., 2009; Nagata et al., 2012**) support the simulation results under euglycemic condition. On the other hand, the simulation results indicated that the inhibition potency of a highly selective SGLT2 inhibitor got greater as plasma glucose increased, and that the difference in FE between inhibitors with different selectivity toward SGLT2 was slight under hyperglycemic condition (**Figs. 6b and 6c**). **Nagata el al. (2012**) reported that, in rats, a highly selective SGLT2 inhibitor, tofogliflozin, and a less selective one, phlorizin, showed 60% and 70% FE, respectively, at the unbound plasma concentrations (tofogliflozin: 196 nM, phlorizin: 1123 nM) under hyperglycemic conditions (300 mg/dl) but showed 20% and 60% FE, respectively, at the same concentrations under euglycemic conditions (100 mg/dl). Moreover, it was reported that the maximum renal glucose clearance induced by a highly selective SGLT2 inhibitor was comparable with that by a less selective inhibitor in db/db mice **(Yamaguchi et al., 2012)**. These facts suggest the validity of the simulation under hyperglycemic conditions.

JPET Fast Forward. Published on February 5, 2013 as DOI: 10.1124/jpet.113.203125
This article has not been copyedited and formatted. The final version may differ from this version.

It was reported that a highly selective SGLT2 inhibitor, dapagliflozin, showed a low risk of hypoglycemia in clinical trials in that the overall incidence of major hypoglycemic events did not exceed 1% and was not significantly increased by dapagliflozin treatment; however, the risk of mild hypoglycemic events was more frequent with dapagliflozin than the placebo (**Musso et al., 2012**). Most SGLT inhibitors in clinical development have high selectivity toward SGLT2; thus, the risk of hypoglycemia for a less selective SGLT inhibitor is not clear but may be higher than for a highly selective one because a less selective one can inhibit not only SGLT2 in the kidney but also SGLT1 in both the kidney and the small intestine. Even if we focus on the action of an SGLT inhibitor only in the kidney, as shown in the simulation study, highly selective SGLT2 inhibition exhibiting mild FE under euglycemic condition (**Fig. 6a**) and great FE equal to a less selective one under hyperglycemic condition (**Figs. 6b and 6c**) would be a preferable characteristic for treating type II diabetes without incurring hypoglycemia because there would be no necessity to reduce blood glucose under euglycemic conditions for the treatment.

Although SGLT1 has been considered to make a minor contribution to renal glucose reabsorption (**Abdul-Ghani et al., 2011**), the complementary role of SGLT1 to SGLT2 has been recently stressed by some researchers (**Hummel et al., 2011; Vallon et al., 2011)** because of the following facts: 1) a highly selective SGLT2 inhibitor, dapagliflozin, caused only less than 50% inhibition of renal glucose reabsorption at the highest dose in healthy subjects (**Komoroski et al., 2009**), and 2) SGLT2 knockout mice excreted approximately 60% of filtered glucose into urine and reabsorbed 40% (**Vallon et al., 2011**). Therefore, the

JPET Fast Forward. Published on February 5, 2013 as DOI: 10.1124/jpet.113.203125
This article has not been copyedited and formatted. The final version may differ from this version.

contribution of SGLT1 to renal glucose reabsorption is an interesting issue for understanding the efficacy of an SGLT inhibitor. The present PK-PD model could suitably express the phenomenon described above by assuming infinite selectivity toward SGLT2 of an SGLT inhibitor, i.e., no inhibition potency to SGLT1, under euglycemic condition as follows: the complete inhibition of SGLT2 caused 55% of FE, and the rest was reabsorbed by SGLT1 (**Fig. 6a**). This means that SGLT1 has transport capacity to reabsorb 45% of the filtered glucose under euglycemic condition when SGLT2 does not contribute to glucose reabsorption. Moreover, the simulation assuming infinite selectivity toward SGLT2 showed that FE was higher under hyperglycemic than euglycemic condition (**Figs. 6b and 6c**). According to the assumptions of the PK-PD model, the difference in FE between eu- and hyperglycemic conditions can be simply explained as follows: FE value under impaired SGLT2 and saturated SGLT1 conditions is estimated by $\left(1-\frac{V_{\max,SGLT1}}{GFR\cdot C_{P,Glc}}\right)\cdot 100$; thus, FE shows a higher value under hyperglycemic condition than euglycemic condition. That would be the reason why a highly selective SGLT2 inhibitor could exhibit potent inhibition for renal glucose reabsorption under hyperglycemic condition without inhibiting SGLT1.For the first time, the present PK-PD model enabled us to express the incomplete inhibition of renal glucose reabsorption by an SGLT2-selective inhibitor (**Komoroski et al., 2009**) and to explain why SGLT2 knockout mice could reabsorb 40% of the filtered glucose (**Vallon et al., 2011**) by considering both SGLT1 and SGLT2 contribution to renal glucose reabsorption; no complicated assumptions were required such as secretion and/or reabsorption of an inhibitor in the proximal tubule (**Liu et al., 2012**). As we previously reported, the

JPET Fast Forward. Published on February 5, 2013 as DOI: 10.1124/jpet.113.203125
This article has not been copyedited and formatted. The final version may differ from this version.

present PK-PD model using rat PD parameters could successfully simulate the excessive urinary glucose excretion in familial renal glycosuria patients with SGLT2 mutation and the mild excretion in glucose-galactose malabsorption patients with SGLT1 mutation **(Yamaguchi et al., 2011)**. The previous simulation can also explain the recent finding of a slight increase of urinary glucose in SGLT1 knockout mice **(Gorboulev et al., 2012)**. It is interesting that the prediction of mouse and human from rat data was successful at a certain level; however, considering the possible species differences in GFR **(Davies and Morris, 1993)** and glucose transport capacity mediated by SGLTs, optimizing the PD parameters for each species would be preferable for a more accurate prediction. A PK-PD model considering only the function of SGLT2 for renal glucose reabsorption was reported to adequately capture the UGE caused by an SGLT2 inhibitor (**Maurer et al., 2011**), and the model can simply describe the effect of an SGLT2 inhibitor. However, the lack of SGLT1 function is likely to limit its usefulness. The present PK-PD model would be suitable for a comprehensive understanding of renal glucose movement and the inhibitory effect of an SGLT inhibitor on renal glucose reabsorption because the model includes the differences between SGLT1 and SGLT2 not only in affinity and transport capacity for glucose but also in inhibition potency of a compound.

In conclusion, the present PK-PD model enabled us to analyze UGE induced by SGLT inhibitors with a wide range of selectivity toward SGLT2, and the estimated in vivo $K_i \times f_u$ values for both SGLT1 and SGLT2 were comparable to the in vitro data. Thus, the model would be useful for predicting UGE caused

by an SGLT inhibitor from in vitro inhibition potency and selectivity toward SGLT2.

Acknowledgements

We thank Dr. Naoki Taka and Dr. Tsutomu Sato (employees of Chugai Pharmaceutical Co., Ltd.) for assistance with synthesizing the test compounds. Dr. Masanori Fukazawa (Chugai Pharmaceutical Co., Ltd.) gave us good comments for preparing the manuscript. We thank Editing Services at Chugai Pharmaceutical Co., Ltd. for editing advice when preparing this paper in English.

Authorship Contributions

Participated in research design: Yamaguchi, Kato, Suzuki, Aso, and Ikeda

Conducted experiments: Yamaguchi, Kato, Suzuki, Hagita, Takada, and Ayabe

Performed data analysis: Yamaguchi and Suzuki

Wrote or contributed to the writing of manuscript: Yamaguchi, Kato, Suzuki, Ishigai, and Ikeda

References

Abdul-Ghani MA, Norton L, and DeFronzo RA (2011) Role of sodium-glucose cotransporter 2 (SGLT2) inhibitors in the treatment of type 2 diabetes. *Endocr Rev* 32: 515–531.

Chasis H, Jolliffe N, and Smith HW (1933) The action of phlorizin on the excretion of glucose, xylose, sucrose, creatinine and urea by man. *J Clin Invest* 12:1083–1090.

Cheng Y and Prusoff WH (1973) Relationship between the inhibition constant (K_i) and the concentration of inhibitor which causes 50 percent inhibition (I_{50}) of an enzymatic reaction. *Biochem Pharmacol* 22: 3099–3108.

Davies B and Morris T (1993) Physiological parameters in laboratory animals and humans. *Pharm Res* 10: 1093–1095.

Deshpande PP, Singh J, Pullockaran A, Kissick T, Ellsworth BA, Gougoutas JZ, Dimarco J, Fakes M, Reyes M, Lai C, Lobinger H, Denzel T, Ermann P, Crispino G, Randazzo M, Gao Z, Randazzo R, Lindrud M, Rosso V, Buono F, Doubleday WW, Leung S, Richberg P, Hughes D, Washburn WN, Meng W, Volk KJ, and Mueller RH (2012) A practical stereoselective synthesis and novel cocrystallizations of an amphiphatic SGLT-2 inhibitor. *Org Process Res Dev* 16: 577–585.

Ellsworth B, Washburn WN, Sher, PM, Wu G, Meng W (2001) Preparation of C-aryl glucoside SGLT-2 inhibitors. *PCT Int Appl*: WO 2001027128 A1 20010419.

Elsas LJ and Rosenberg LE (1969) Familial renal glycosuria: a genetic reappraisal of hexose transport by

kidney and intestine. *J Clin Invest* 48: 1845–1854.

Fujimori Y, Katsuno K, Ojima K, Nakashima I, Nakano S, Ishikawa-Takemura Y, Kusama H, and Isaji M. (2009) Sergliflozin etabonate, a selective SGLT2 inhibitor, improves glycemic control in streptozotocin-induced diabetic rats and Zucker fatty rats. *Eur J Pharmacol* 609: 148–154.Hediger MA and Rhoads DB (1994) Molecular physiology of sodium-glucose cotransporters. *Physiol Rev* 74: 993–1026.

Gorboulev V, Schürmann A, Vallon V, Kipp H, Jaschke A, Klessen D, Friedrich A, Scherneck S, Rieg T, Cunard R, Veyhl-Wichmann M, Srinivasan A, Balen D, Breljak D, Rexhepaj, Parker HE, Gribble FM, Reimann F, Lang F, Wiese S, Sabolic I, Sendtner M, and Koepsell H (2012) Na+-D-glucose cotransporter SGLT1 is pivotal for intestinal glucose absorption and glucose-dependent incretin secretion. Diabetes 61: 187–196.

Hummel CS, Lu C, Loo DD, Hirayama BA, Voss AA, and Wright EM (2011) Glucose transport by human renal Na+/D-glucose cotransporters SGLT1 and SGLT2. *Am J Physiol Cell Physiol* 300: C14–C21.

Hussey EK, Dobbins RL, Stoltz RR, Stockman NL, O'Connor-Semmes RL, Kapur A, Murray SC, Layko D, and Nunez DJ (2010) Multiple-dose pharmacokinetics and pharmacodynamics of sergliflozin etabonate, a novel inhibitor of glucose reabsorption, in healthy overweight and obese subjects: a randomized double-blind study. *J Clin Pharmacol* 50: 636–646.

Jabbour SA and Goldstein BJ (2008) Sodium-glucose co-transporter 2 inhibitors: blocking renal tubular

reabsorption of glucose to improve glycaemic control in patients with diabetes. *Int J Clin Pract* 62: 1279 –1284.

Jurczak MJ, Lee HY, Birkenfeld AL, Jornayvaz FR, Frederick DW, Pongratz RL, Zhao X, Moeckel GW, Samuel VT, Whaley JM, Shulman GI, and Kibbey RG (2011) SGLT2 deletion improves glucose homeostasis and preserves pancreatic beta-cell function. *Diabetes* 60: 890–898.

Katsuno K, Fujimori Y, Takemura Y, Hiratochi M, Itoh F, Komatsu Y, Fujikura H, and Isaji M (2007) Sergliflozin, a novel selective inhibitor of low-affinity sodium glucose cotransporter (SGLT2), validates the critical role of SGLT2 in renal glucose reabsorption and modulates plasma glucose level. *J Pharmacol Exp Ther* 320:323–330.

Kipnes MS (2011) Sodium-glucose cotransporter 2 inhibitors in the treatment of type 2 diabetes: a review of phase II and III trials. *Clin Invest* 1: 145–156.

Komoroski B, Vachharajani N, Boulton D, Kornhauser D, Geraldes M, Li L, and Pfister M (2009) Dapagliflozin, a novel SGLT2 inhibitor, induces dose-dependent glucosuria in healthy subjects. *Clin Pharmacol Ther* 85: 520–526.

List FL and Whaley JM (2011) Glucose dynamics and mechanistic implications of SGLT2 inhibitors in animals and humans. *Kidney Int* 79: S20–S27.

Liu JJ, Lee TW, and DeFronzo RA (2012) Why do SGLT2 inhibitors inhibit only 30–50% of renal glucose reabsorption in humans? *Diabetes* 61: 2199–2204.

Magen D, Sprecher E, Zelikovic I, and Skorecki K (2005) A novel missense mutation in SLC5A2 encoding SGLT2 underlies autosomal-recessive renal glucosuria and aminoaciduria. *Kidney Int* 67: 34–41.

Maurer TS, Ghosh A, Haddish-Berhane N, Sawant-Basak A, Boustany-Kari CM, She L, Leininger MT, Zhu T, Tugnait M, Yang X, Kimoto E, Mascitti V, and Robinson RP (2011) Pharmacodynamic model of sodium–glucose transporter 2 (SGLT2) inhibition: implications for quantitative translational pharmacology. *AAPS J* 13: 576–584.

Musso G, Gambino R, Cassader M, and Pagano G (2012) A novel approach to control hyperglycemia in type 2 diabetes: Sodium glucose co-transport (SGLT) inhibitors: systematic review and meta-analysis of randomized trials. *Ann Med* 44: 375–393.

Nagata T, Fukazawa M, Honda K, Yata T, Kawai M, Yamane M, Murao N, Yamaguchi K, Kato M, Mitsui T, Suzuki Y, Ikeda S, and Kawabe Y (2012) Selective SGLT2 inhibition by tofogliflozin reduces renal glucose reabsorption under hyperglycemic but not under hypo- or euglycemic conditions in rats. *Am J Physiol Endocrinol Metab* doi: 10.1152/ajpendo.00545.2012.

Ohtake Y, Sato T, Kobayashi T, Nishimoto M, Taka N, Takano K, Yamamoto K, Ohmori M, Yamaguchi M, Takami K, Yeu SY, Ahn KH, Matsuoka H, Morikawa K, Suzuki M, Hagita H, Ozawa K, Yamaguchi K, Kato M, and Ikeda S (2012) Discovery of tofogliflozin, a novel *C*-arylglucoside with an *O*-spiroketal ring system, as a highly selective sodium glucose cotransporter 2 (SGLT2) inhibitor for the treatment of type 2 diabetes. *J Med Chem* 55: 7828–7840.

Oku A, Ueta K, Arakawa K, Ishihara T, Nawano M, Kuronuma Y, Matsumoto M, Saito A, Tsujihara K, Anai M, Asano T, Kanai Y, and Endou H (1999) T-1095, an inhibitor of renal Na+-glucose cotransporters, may provide a novel approach to treating diabetes. *Diabetes* 48:1794–1800.

Oku A, Ueta K, Nawano M, Arakawa K, Kano-Ishihara T, Matsumoto M, Saito A, Tsujihara K, Anai M, and Asano T (2000) Antidiabetic effect of T-1095, an inhibitor of Na^+-glucose cotransporter, in neonatally streptozotocin-treated rats. *Eur J Pharmacol* 391: 183–192.

Oulianova N and Berteloot A (1996) Sugar transport heterogeneity in the kidney: two independent transporters or different transport modes through an oligomeric Protein? 1. Glucose transport studies. *J Membr Biol* 153: 181–194.

Rossetti L, Smith D, Shulman GI, Papachristou D, and DeFronzo RA (1987) Correction of hyperglycemia with phlorizin normalizes tissue sensitivity to insulin in diabetic rats. *J Clin Invest* 79: 1510–1515.

Silverman M, Aganon MA, and Chinard FP (1970) D-Glucose interactions with renal tubule cell surfaces. *Am J Physiol* 218: 735–742.

Suzuki M, Honda K, Fukazawa M, Ozawa K, Hagita H, Kawai T, Takeda M, Yata T, Kawai M, Fukuzawa T, Kobayashi T, Sato T, Kawabe Y, and Ikeda S (2012) Tofogliflozin, a potent and highly specific sodium/glucose cotransporter 2 inhibitor, improves glycemic control in diabetic rats and mice. *J Pharmcol Exp Ther* 341: 692–701.

Turner RJ and Moran A (1982) Heterogeneity of sodium-dependent D-glucose transport sites along the

proximal tubule: evidence from vesicle studies. *Am J Physiol* 242: F406–F414.

Vallon V, Platt KA, Cunard R, Schroth J, Whaley J, Thomson SC, Koepsell H, and Rieg T (2011) SGLT2 mediates glucose reabsorption in the early proximal tubule. *J Am Soc Nephrol* 22: 104–112.

Wright EM (2001) Renal Na^+-glucose cotransporters. *Am J Physiol Renal Physiol* 280: F10–F18.

Yamaguchi K, Kato M, Suzuki M, Asanuma K, Aso Y, Ikeda S, and Ishigai M (2011) Pharmacokinetic and pharmacodynamic modeling of the effect of an sodium-glucose cotransporter inhibitor, phlorizin, on renal glucose transport in rats. *Drug Metab Dispos* 39: 1801–1807.

Yamaguchi K, Kato M, Ozawa K, Kawai T, Yata T, Aso Y, Ishigai M, and Ikeda S (2012) Pharmacokinetic and pharmacodynamic modeling for the effect of SGLT inhibitors on blood glucose level and renal glucose excretion in db/db mice. *J Pharm Sci* 101: 4347–4356.

Yamaoka K, Tanigawara Y, Nakagawa T, and Uno T (1981) A pharmacokinetic analysis program (MULTI) for microcomputer. *J Pharmacobio-dyn* 4: 879–885.

Footnotes

The authors of this work are employees of Chugai Pharmaceutical or Chugai Research Institute for Medical Science and have not received financial support from any other institution.

Please send reprint requests to: Koji Yamaguchi, PhD

Research Division, Chugai Pharmaceutical Co., Ltd., 1-135 Komakado, Gotemba, Shizuoka 412-8513, Japan

E-mail: yamaguchikuj@chugai-pharm.co.jp

JPET Fast Forward. Published on February 5, 2013 as DOI: 10.1124/jpet.113.203125
This article has not been copyedited and formatted. The final version may differ from this version.

Legends for figures

Figure 1. Chemical structures of SGLT inhibitors: tofogliflozin (a), BMS (b), sergliflozin (c), sergliflozin-A (d), T-1095 (e), and T-1095A (f).

Figure 2. Schematic representation of a PK-PD model for the effect of an SGLT inhibitor on renal glucose transport.

Figure 3. Relationship between $CL_{R,Glc}$ and plasma concentration of tofogliflozin (a), BMS (b), sergliflozin-A (c), T-1095A (d), or phlorizin (e). Symbols indicate data from intravenous (circles) or oral (crosses) administration of a compound. Lines show the regression curves estimated using the plots of $CL_{R,Glc}$ that were 50–400 ml/h/kg. Slope means the slope of regression curve. Data of phlorizin was cited from a previous report (Yamaguchi et al., 2011).

Figure 4. Time courses of plasma concentrations for glucose and compound [tofogliflozin (a), BMS (b), sergliflozin-A (c), and T-1095A (d)] and of cumulative glucose excreted into urine after intravenous administration of each test compound. PC: plasma concentration of compound, PG: plasma concentration of glucose, GE: cumulative glucose excreted into urine. Open circle and error bar show the mean value of observed data (n=3 or 4) and the corresponding SD, respectively. Lines for PC and PG were simulated using PK parameters based on the 2-compartment model and linear interpolation, respectively. Line for GE was obtained by curve-fitting.

Figure 5. In vitro–in vivo relationships of rat K_i of SGLT inhibitors for SGLT1 and SGLT2 (a) and of

JPET Fast Forward. Published on February 5, 2013 as DOI: 10.1124/jpet.113.203125
This article has not been copyedited and formatted. The final version may differ from this version.

selectivity toward SGLT2 (b). The in vivo $K_i \times f_u$ values were estimated by the present PK-PD analysis. The in vitro K_i values were calculated from the in vitro IC_{50} values using the Cheng-Prusoff relationship. In panel a, the line passing through the origin shows the line of identity, and broken lines show 5-fold difference. In panel b, the line shows the regression-curve. 1: tofogliflozin, 2: BMS, 3: sergliflozin-A, 4: phlorizin.

Figure 6. Relationship between plasma drug concentration and FE. FE was simulated based on the present PK-PD model, using rat PD parameters and assuming $K_{i,SGLT2}$ value of 1 nM and different selectivity toward SGLT2 (1, 10, 100, 1000, and infinity) with plasma glucose levels of 1 mg/ml (a), 2 mg/ml (b), or 3 mg/ml (c). A static drug concentration was used for the simulation.

JPET Fast Forward. Published on February 5, 2013 as DOI: 10.1124/jpet.113.203125
This article has not been copyedited and formatted. The final version may differ from this version.

Table 1. Composition of dosing solution and amount of dose for test compounds.

Compound	Administration route	Vehicle	Dose (mg/kg)
Tofogliflozin	Intravenous	PEG400/saline (4:6, v/v)	3
	Oral	0.5% (w/v) carboxymethylcellulose	10
BMS	Intravenous	PEG400/saline (4:6, v/v)	3
	Oral	0.5% (w/v) carboxymethylcellulose	10
Sergliflozin	Intravenous	PEG400/saline (1:1, v/v)	10
	Oral	0.5% (w/v) carboxymethylcellulose	400
T-1095	Intravenous	PEG400/saline (1:1, v/v)	10

JPET Fast Forward. Published on February 5, 2013 as DOI: 10.1124/jpet.113.203125
This article has not been copyedited and formatted. The final version may differ from this version.

Table 2. Pharmacodynamic and biochemical parameters relating to rat renal glucose transport. The values were cited from the previous report (Yamaguchi et al., 2011).

GFR	$V_{max,SGLT1}$	$V_{max,SGLT2}$	$K_{m,SGLT1}$		$K_{m,SGLT2}$	
(ml/h/kg)	(mg/h/kg)	(mg/h/kg)	(mg/ml)	(mM)	(mg/ml)	(mM)
558	256	1392	0.016	0.0862	0.197	1.09

Table 3. In vitro IC_{50} and in vivo K_i values for glucose transport mediated by SGLT1 and SGLT2, and plasma protein binding of test compounds. The values in parentheses are CV of the estimates. In vitro IC_{50} value of each compound was calculated from 2 to 4 independent experiments using CHO expressing mSGLT1 and mSGLT2 or COS-7 expressing rSGLT1 and rSGLT2. In vivo K_i values were estimated from the PK-PD analysis based on a nonlinear parallel tube model. The values in parentheses are CV of the estimate.

Compound	In vitro parameter							In vivo parameter		
	Mouse			Rat				Rat		
	IC_{50} (nM)		Selectivity toward SGLT2	IC_{50} (nM)		Selectivity toward SGLT2	f_u	Rat K_i (nM)		Selectivity toward SGLT2
	SGLT1	SGLT2	Using IC_{50}	SGLT1	SGLT2	Using IC_{50}		SGLT1	SGLT2	Using K_i
Tofogliflozin	1,800 [a]	5.0 [a]	360 [a]	8,200 [a]	15 [a]	560 [a]	0.17 [a]	30,000 (297%)	18 (12%)	1,700
BMS	6,900 (5%)	13 (49%)	550	27,000 [c] (15%)	26 [c] (4%)	1,000	0.139 (4%)	38,000 (38%)	31 (6%)	1,200
Sergliflozin-A	990 (20%)	6.8 (7%)	150	3,000 [c] (12%)	17 [c] (7%)	170	0.133 (3%)	2,700 (5%)	65 (7%)	41
T-1095A	96 (20%)	6.3 (8%)	15	NE	NE	NC	0.069 (6%)	19 (69%)	28 (37%)	0.7
Phlorizin	310 [a]	17 [a]	19 [a]	970 [a]	48 [a]	20 [a]	0.337 [b]	67 [b]	250 [b]	0.3

NE: not examined. NC: not calculated. [a] Cited from **Suzuki et al., 2012**. [b] Cited from **Yamaguchi et al., 2011**. [c] n=2.

JPET Fast Forward. Published on February 5, 2013 as DOI: 10.1124/jpet.113.203125
This article has not been copyedited and formatted. The final version may differ from this version.

Table 4. Pharmacokinetic parameters of test compounds after intravenous administration. PK parameters were estimated based on a 2-compartment model using WinNonlin Ver. 5.0 software. The values in parentheses are CV of the estimate.

Compound	V_1 (ml/kg)	k_{10} (/h)	k_{12} (/h)	k_{21} (/h)
Tofogliflozin	498 (23%)	2.40 (21%)	3.62 (34%)	1.08 (24%)
BMS	560 (19%)	1.30 (18%)	3.33 (38%)	1.39 (28%)
Sergliflozin-A	1820 (10%)	1.88 (10%)	1.70 (32%)	1.50 (29%)
T-1095A	1800 (15%)	1.30 (18%)	2.30 (33%)	0.965 (39%)

Figure 1

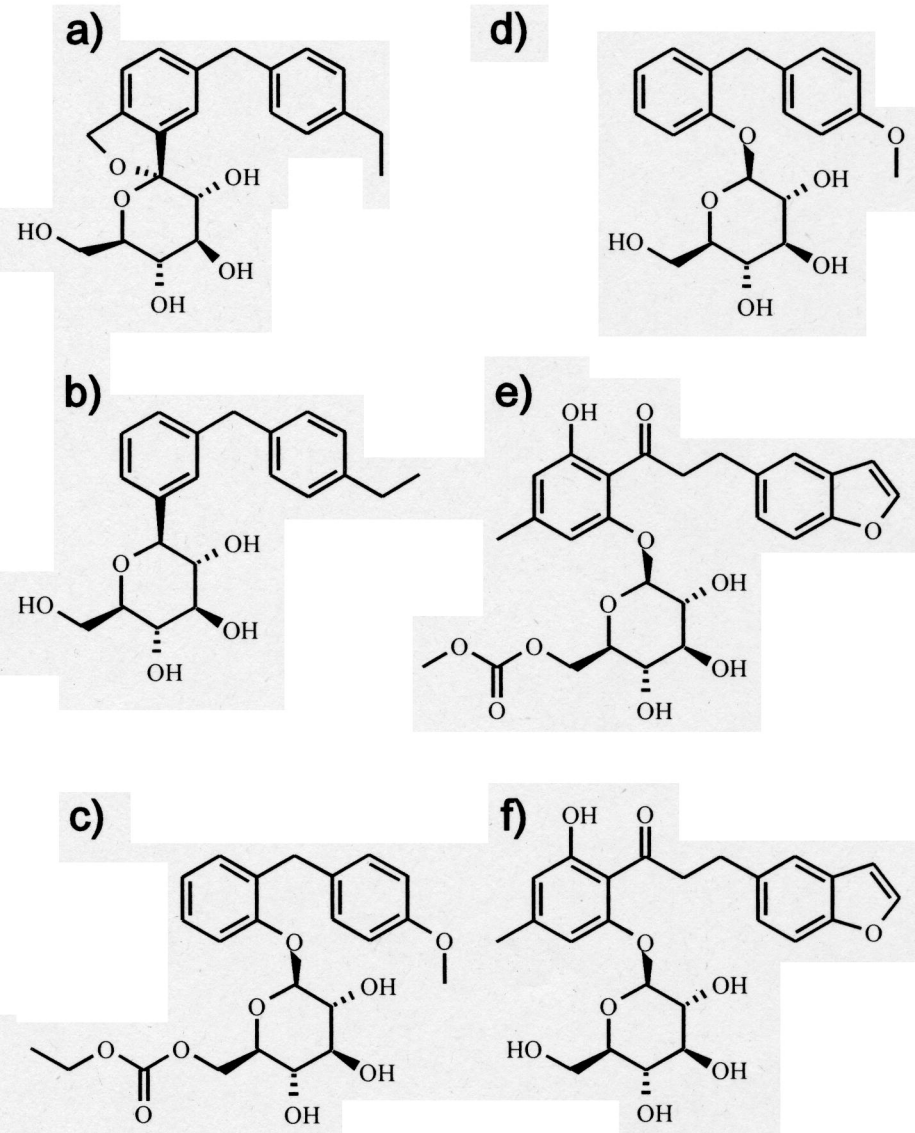

Figure 2

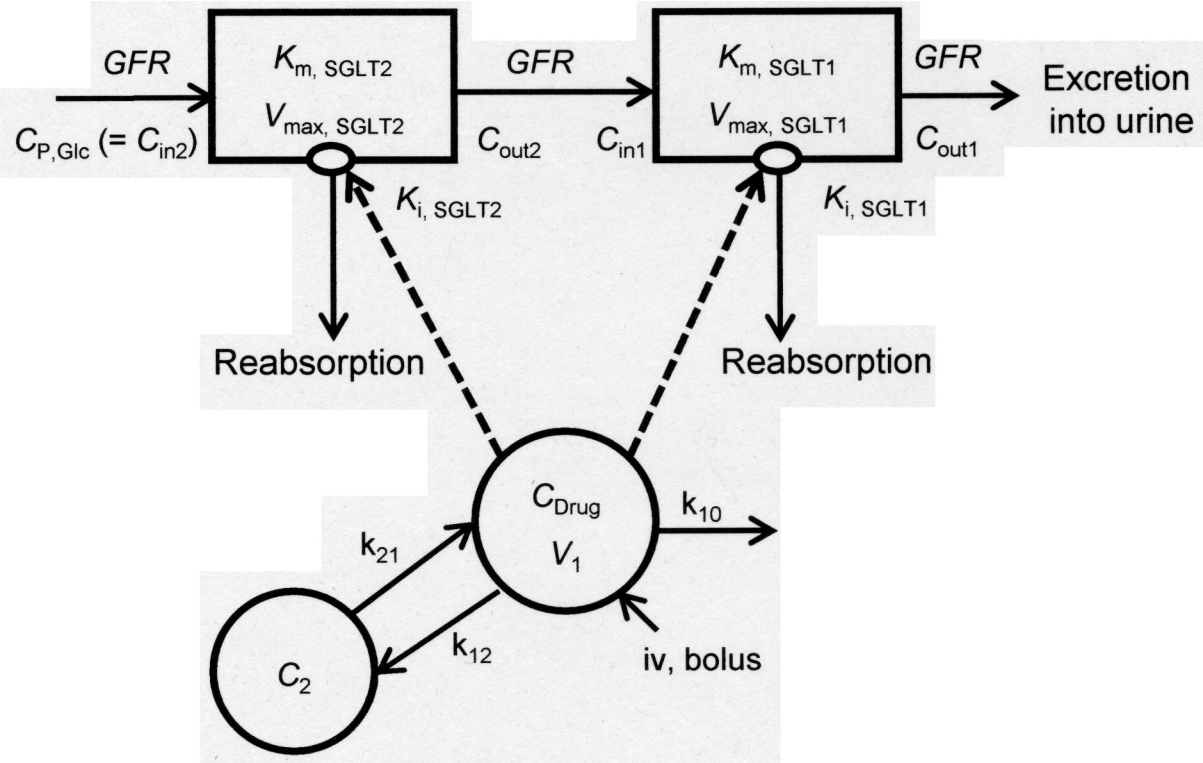
GFR
$K_{m,\ SGLT2}$
$V_{max,\ SGLT2}$
GFR
$K_{m,\ SGLT1}$
$V_{max,\ SGLT1}$
GFR
Excretion into urine
$C_{P,Glc}$ (= C_{in2})
C_{out2}
C_{in1}
C_{out1}
$K_{i,\ SGLT2}$
$K_{i,\ SGLT1}$
Reabsorption
Reabsorption
C_{Drug}
V_1
k_{10}
k_{21}
k_{12}
C_2
iv, bolus

Figure 3

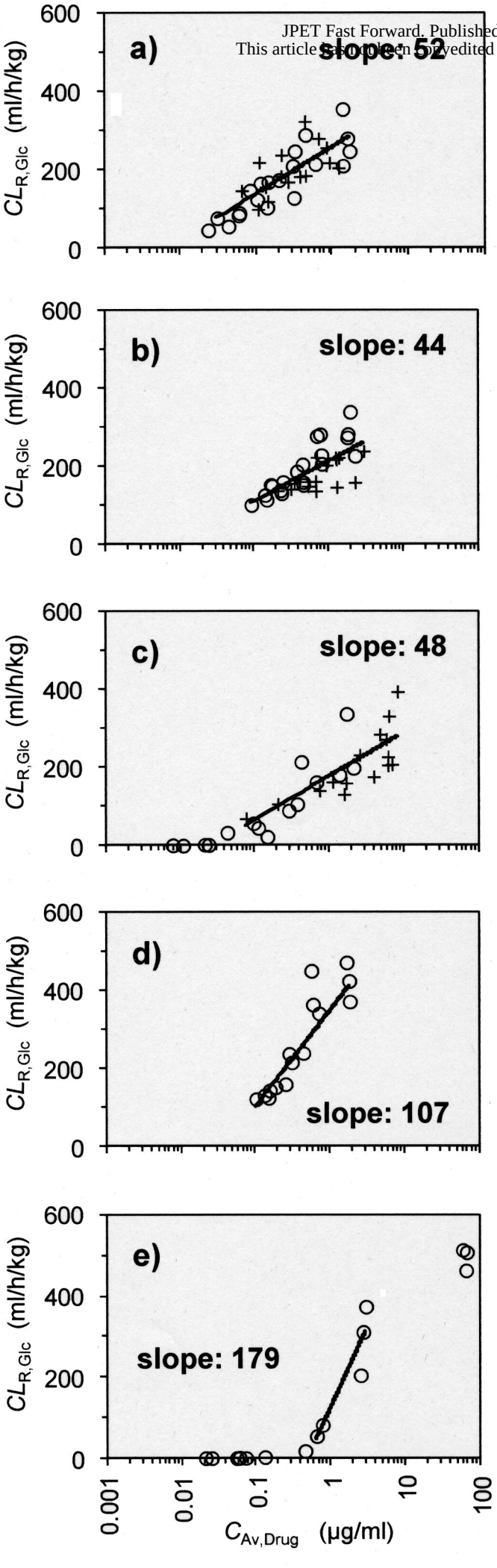

Figure 4

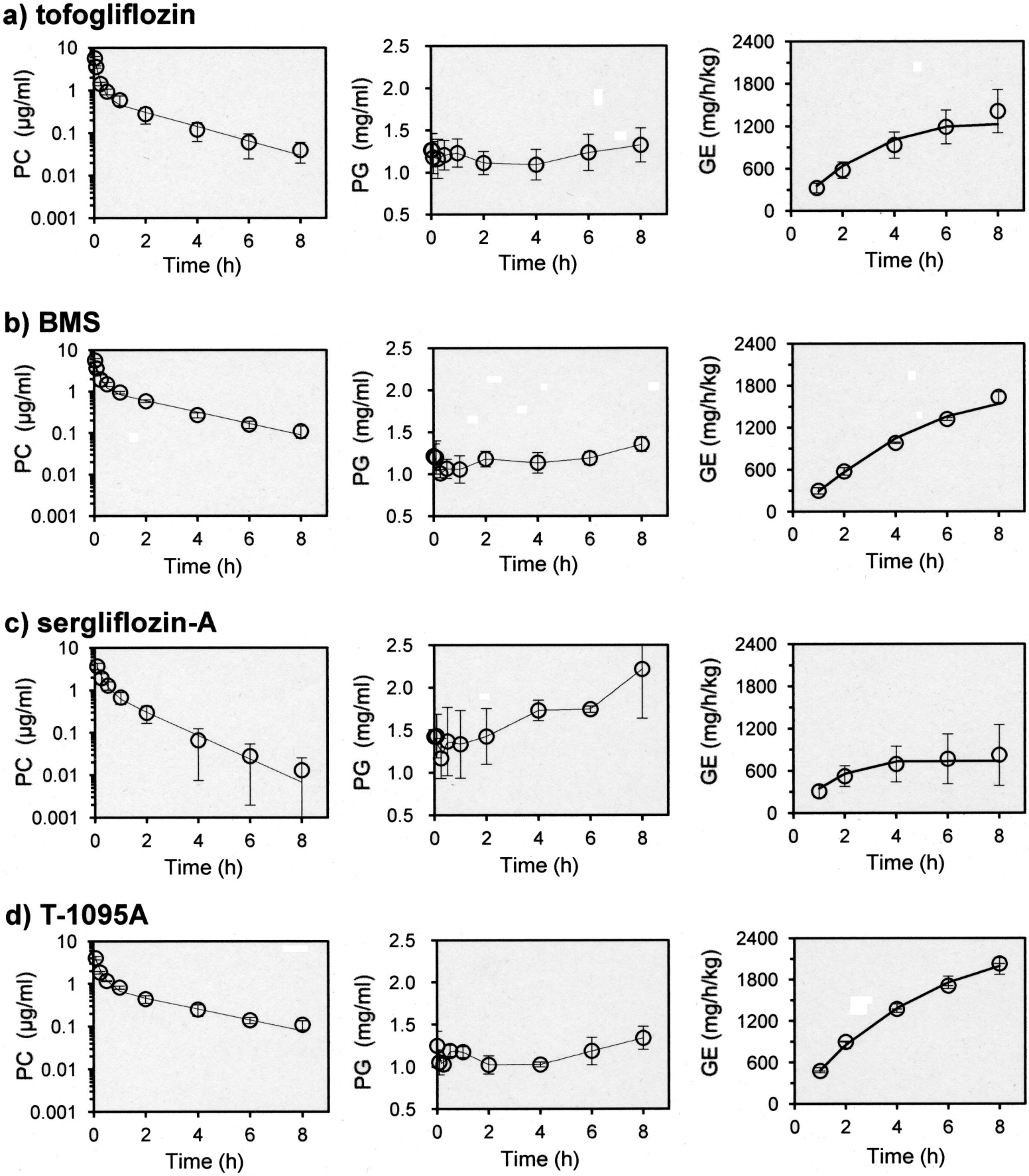
a) tofogliflozin
b) BMS
c) sergliflozin-A
d) T-1095A
PC (μg/ml)
PG (mg/ml)
GE (mg/h/kg)
Time (h)
10
1
0.1
0.01
0.001
2.5
2.0
1.5
1.0
0.5
2400
1800
1200
600
0
0
2
4
6
8

Figure 5

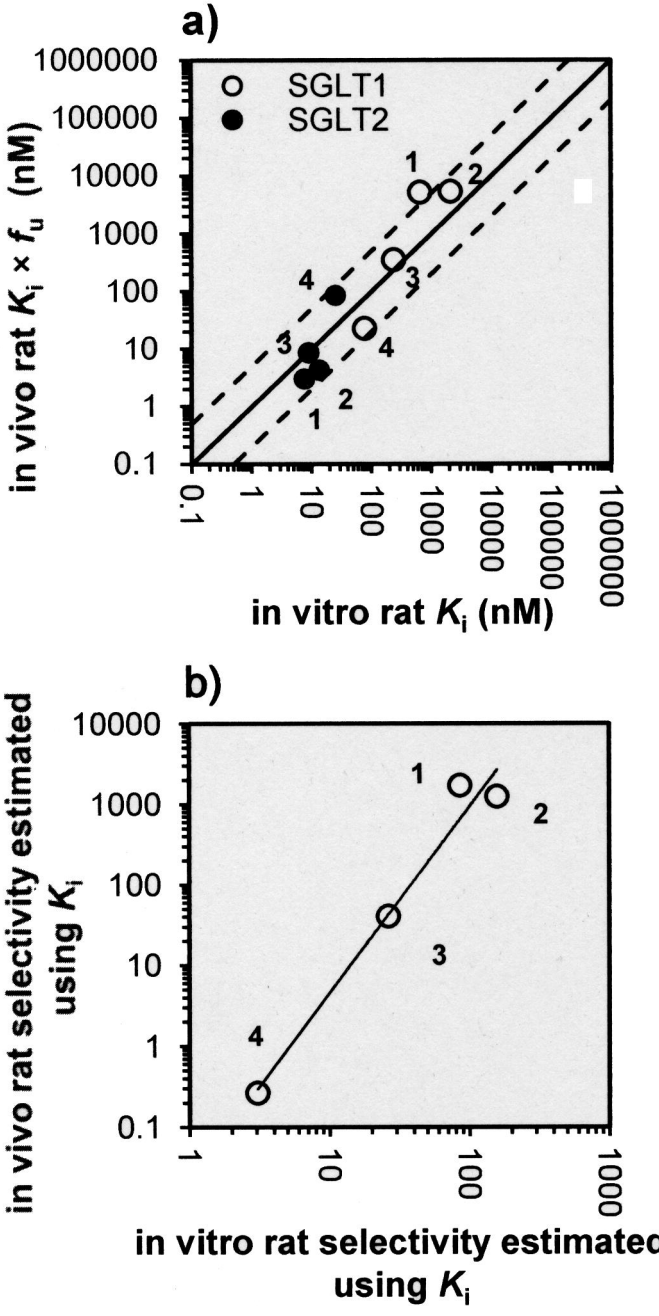
a)
SGLT1
SGLT2
in vivo rat $K_i \times f_u$ (nM)
in vitro rat K_i (nM)
1000000
100000
10000
1000
100
10
1
0.1
b)
in vivo rat selectivity estimated using K_i
in vitro rat selectivity estimated using K_i
10000
1000
100
10
1
0.1

Figure 6

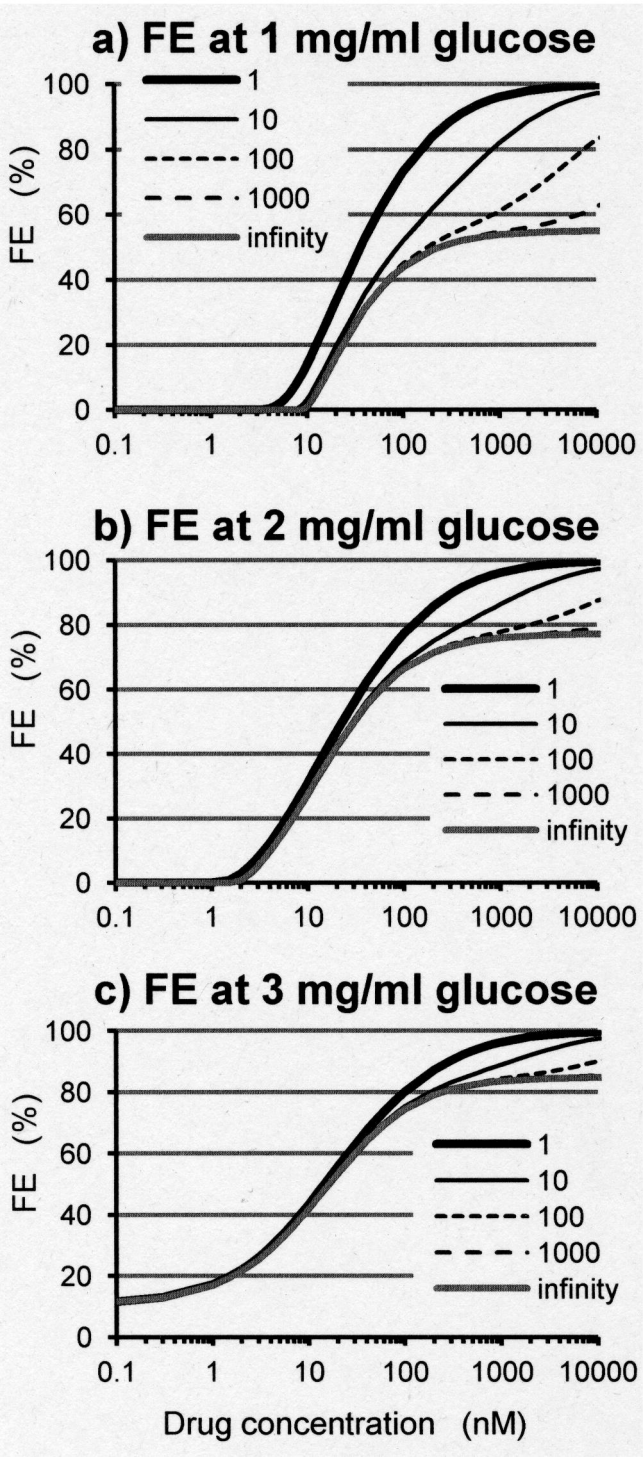
a) FE at 1 mg/ml glucose
FE (%)
100
80
60
40
20
0
1
10
100
1000
infinity
0.1
1
10
100
1000
10000
b) FE at 2 mg/ml glucose
FE (%)
100
80
60
40
20
0
1
10
100
1000
infinity
0.1
1
10
100
1000
10000
c) FE at 3 mg/ml glucose
FE (%)
100
80
60
40
20
0
1
10
100
1000
infinity
0.1
1
10
100
1000
10000
Drug concentration (nM)